

expected to have different isotopic compositions. Experiments<sup>16</sup> have shown that spinel and pyroxene have higher minimum melting temperatures in this system than melilite and anorthite. Observations<sup>13</sup> show that the spinel and pyroxene of Ca-rich inclusions have greater concentrations of excess <sup>16</sup>O than melilite, by about a factor of four. This could be explained by a partial melting of the inclusions at a time when there was less excess <sup>16</sup>O in the ambient gas than in the inclusion. On the same grounds, one could expect deviations from the Mg–Al isochron to occur. But, the higher melting point phases (spinel, pyroxene) have such small Al/Mg ratios that relatively large differences in their initial <sup>26</sup>Al/<sup>27</sup>Al ratios would, considering the experimental uncertainty<sup>2</sup>, be unobservable. Thus, the determination of the source of the Mg and O anomalies will be difficult since we may not see the original distribution of <sup>26</sup>Al and excess <sup>16</sup>O.

One other distinction remains between the Mg and O anomalies. While the <sup>26</sup>Al has to be associated with a nucleosynthetic event that occurred within a few million years of the Solar System's formation, the observed excess <sup>16</sup>O does not. Since the (C) and (O) zones produce excess <sup>16</sup>O, either 'old' presolar grains or 'last-event' supernova grains could have carried excess <sup>16</sup>O into the presolar nebula. But, if grains cannot form in supernova ejecta, the only remaining way, in our scenario, to inject excess <sup>16</sup>O is through last-event supernova gas.

The <sup>22</sup>Ne anomaly<sup>14</sup> observed in CI chondrites may have been produced by 2.6 yr <sup>22</sup>Na-bearing presolar grains condensed in the (He) zone<sup>19</sup>. In the solar nebula these grains vaporise if  $T_{\max} > 1,000$  K. But evidence<sup>20</sup> suggests that CI chondrites may have formed in nebular regions where  $T_{\max} < 400$  K; if decay-produced <sup>22</sup>Ne can be retained in or on these grains at this temperature, incorporation of excess <sup>22</sup>Ne into CI chondrites may occur. But, irradiation<sup>17</sup> in the early solar nebula could also produce excess <sup>22</sup>Ne with energy requirements far less stringent than those for the production of <sup>26</sup>Mg by irradiation.

What minerals could survive in the presolar nebula if the composition was solar except for a C/O ratio  $> 1$ ? Enstatite chondrites apparently condensed in such a region<sup>21</sup>. Unfortunately, less is known about the mineralogical history of enstatite chondrites, so no limits on  $T_{\max}$  can at present be imposed. Calculations<sup>11</sup> show that if  $T_{\max} > 2,025, 1,930, 1,745, 1,458, 1,400$  and  $1,390$  K, respectively, TiC, C, SiC, Fe<sub>3</sub>C, AlN and CaS could survive: all of these phases can be condensed in at least two supernova zones (if C/O  $> 1$  in the appropriate supernova zones). Thus, C, N, S and Fe, in addition to Mg, Si, Ca and Ti, isotopic measurements could potentially be key indicators of which supernova zones have been sampled. The C<sup>12</sup>/C<sup>13</sup> ratio could prove very important in this respect, since this ratio should be less than its solar value if the (H) zone is responsible, while if presolar grains from the (He) and/or (C) zones are incorporated in enstatite chondrites this ratio should be greater than its solar value.

Before the discovery of the <sup>26</sup>Mg anomaly, it was thought that

the last nucleosynthetic event affecting the Solar System occurred about 10<sup>8</sup> yr before its formation<sup>22</sup>, which is the interval between the production of the r-process radioactive parents (<sup>129</sup>I, <sup>244</sup>Pu) of Xe and the retention of daughter Xe in the meteorites. Assuming that the anomalous <sup>26</sup>Mg is the *in situ* decay product of <sup>26</sup>Al, the Mg timescale is about 10<sup>6</sup> yr. There are at least two explanations for this discrepancy. First, <sup>26</sup>Al, <sup>129</sup>I and <sup>244</sup>Pu may not have been produced in the same nucleosynthetic event, but in separate events 10<sup>8</sup> yr apart. The latter event made <sup>26</sup>Al, but no r-process nuclei (or at least its r-process material did not get into the solar nebula). The incorporation of Al, I and Pu occurred about 10<sup>6</sup> yr later. The second explanation is that these three nuclei were all made in the same (last) event, but somehow Xe was unable to be retained by meteorites until 10<sup>8</sup> yr later, possibly because this region of the presolar nebula or the meteorite parent bodies remained too hot. A search for <sup>235</sup>U anomalies due to the decay of <sup>247</sup>Cm might resolve this problem<sup>23</sup>. <sup>247</sup>Cm (half life  $1.54 \times 10^7$  yr), <sup>129</sup>I ( $1.7 \times 10^7$  yr) and <sup>244</sup>Pu ( $8.3 \times 10^7$  yr) are all r-process nuclei. The U timescale's turning out to be of the order of the Xe timescale would be evidence in favour of the first possibility since U is a refractory element and does not diffuse out of meteoritic minerals as readily as gaseous Xe.

It seems, therefore, that a last-event supernova provides a consistent explanation of the observed isotopic anomalies. Condensation sequences for supernova ejecta imply that presolar grains may be a useful part of this picture.

We thank E. Anders, D. Arnett, R. Clayton, S. Falk and J. Truran for useful discussions. J.M.L. expresses appreciation for the hospitality of both the Institute of Astronomy, Cambridge, England, and NORDITA, Copenhagen, Denmark, where part of this research was done. This work was supported in part by the US NSF (J.M.L., D.N.S.), NASA (J.M.L., D.N.S., L.G.) and by the Alfred P. Sloan Foundation (L.G.).

Received 29 April; accepted 27 June 1977.

<sup>1</sup> Gray, C. M. & Compston, W. *Nature* **251**, 495 (1974).

<sup>2</sup> Lee, T., Papanastassiou, D. A. & Wasserburg, G. J. *Astrophys. J. Lett.* **211**, L107 (1977).

<sup>3</sup> Schramm, D. N. *Astrophys. Space Sci.* **13**, 249 (1971); *Bull. Am. astr. Soc.*, Hawaii (1977).

<sup>4</sup> Sabu, D. D. & Manuel, O. K. *Nature* **262**, 28 (1976); Cameron, A. G. W. & Truran, J. W. *Icarus* **30**, 447 (1977).

<sup>5</sup> Woodward, P. R. *Astrophys. J.* **207**, 484 (1976).

<sup>6</sup> Schramm, D. N. & Arnett, W. D. *Mercury* **4**, 16 (1975).

<sup>7</sup> Howard, W. M., Arnett, W. D. & Clayton, D. D. *Astrophys. J.* **165**, 495 (1971).

<sup>8</sup> Pardo, R. C., Couch, R. G. & Arnett, W. D. *Astrophys. J.* **191**, 711 (1974).

<sup>9</sup> Woosley, S. E., Arnett, W. D. & Clayton, D. D. *Astrophys. J. Suppl.* **26**, 231 (1973).

<sup>10</sup> Couch, R. G., Schmeidekamp, A. B. & Arnett, W. D. *Astrophys. J.* **190**, 95 (1974).

<sup>11</sup> Lattimer, J. M., Schramm, D. N. & Grossman, L. *Astrophys. J.* (1978).

<sup>12</sup> Cameron, A. G. W. in *Explosive Nucleosynthesis* (eds Schramm, D. N. & Arnett, W. D.) (University of Texas Press, Austin, 1973).

<sup>13</sup> Clayton, R. N., Onuma, N., Grossman, L. & Mayeda, T. K. *Earth planet. Sci. Lett.* **34**, 209 (1977).

<sup>14</sup> Blander, M. & Fuchs, L. H. *Geochim. cosmochim. Acta* **39**, 1605 (1975).

<sup>15</sup> Grossman, L. & Ganapathy, R. *Geochim. cosmochim. Acta* **40**, 331 (1976).

<sup>16</sup> Seitz, M. G. & Kushiro, I. *Science* **183**, 954 (1974).

<sup>17</sup> Black, D. C. *Geochim. cosmochim. Acta* **136**, 377 (1972).

<sup>18</sup> Eberhardt, P. *Earth planet. Sci. Lett.* **24**, 182 (1974).

<sup>19</sup> Clayton, D. D. *Nature* **257**, 36 (1975).

<sup>20</sup> Grossman, L. *Scient. Am.* **232**, 30 (1975).

<sup>21</sup> Larimer, J. W. *Geochim. cosmochim. Acta* **39**, 389 (1975).

<sup>22</sup> Schramm, D. N. & Wasserburg, G. J. *Astrophys. J.* **162**, 57 (1970).

<sup>23</sup> Blake, J. B. & Schramm, D. N. *Nature phys. Sci.* **243**, 138 (1973).

## Three-dimensional model of membrane-bound ribosomes obtained by electron microscopy

P. N. T. Unwin

MRC Laboratory of Molecular Biology, Hills Road, Cambridge, UK

*A low-resolution three-dimensional map has been obtained from crystalline arrays of membrane-bound eukaryotic ribosomes. It shows both ribosomal subunits to be adjacent to the membrane surface, attached to it by a part protruding from the large subunit.*

Most eukaryotic cells have two populations of actively synthesising ribosomes which are distinguishable morphologically according to whether they exist free in the cytoplasm or are bound to membranes, normally the endoplasmic reticulum. In general, the two populations synthesise different sets of proteins. One function of membrane-bound ribosomes, originally discovered from

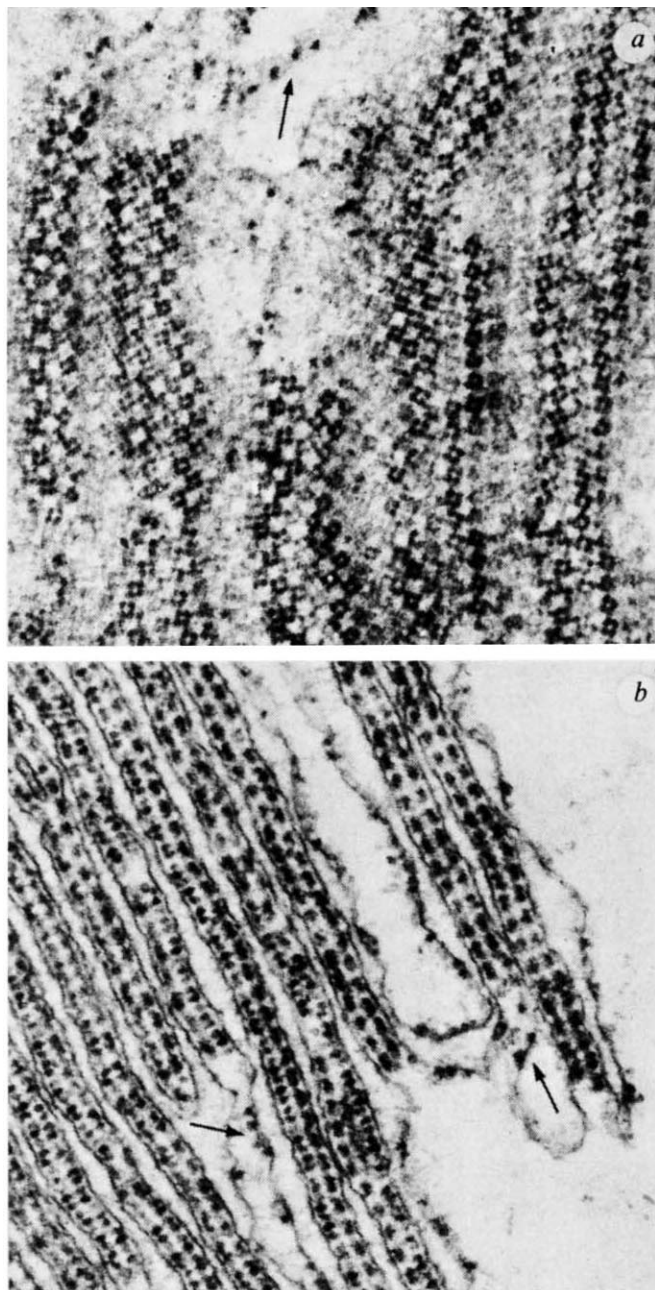


**Fig. 1** Organisation of crystalline ribosomes and membranes as in the oocyte of *Lacerta sicula* during winter. *a*, Face-on view; *b*, edge-on view. Membrane-bound ribosomes which are separate from those in the crystals (arrows) are also evident ( $\times 50,000$ ). To bring out details clearly, the ribosome-membrane complexes have been isolated from the cytoplasm and suspended in 100 mM KCl, 5 mM  $MgCl_2$ , 0.25 M sucrose, 50 mM triethanolamine-HCl, pH 7.6. All thin sections were prepared by fixing in glutaraldehyde, post-fixing in  $OsO_4$ , embedding in Araldite, then staining after cutting with uranyl acetate and lead citrate.

experiments with secretory cells<sup>1</sup>, is to synthesise proteins for export from the cell. These proteins are vectorially discharged through the membrane during synthesis<sup>2</sup>.

Ribosomes are attached to the membranes by two types of interaction<sup>3</sup>; one is sensitive to ionic strength and the other to the antibiotic puromycin. The salt-sensitive interaction occurs directly between the large ribosomal subunit and the membrane, but its significance is not yet understood. The puromycin-sensitive interaction is indirect and is thought to be due to an anchoring effect by the membrane on the nascent polypeptide chain. It is therefore associated with proteins which are to be transferred across

the membrane. Recent findings indicate that the specificity for the interaction between the nascent polypeptide and the membrane resides in the amino-terminal sequence of the protein<sup>4-7</sup>.

It is generally assumed that the large ribosomal subunit lies between the small subunit and the membrane surface<sup>8,9</sup> and that the protein being synthesised passes into and through the membrane through a protected region<sup>10,11</sup> within the large subunit. But the electron microscopical and biochemical experiments on which these ideas are based do not provide definitive evidence, and the exact configuration of the ribosome with respect to the membrane is uncertain.

This study is based on a three-dimensional analysis of crystalline arrays of ribosomes which bind to membranes through a salt-sensitive linkage. The commonly assumed configuration is not confirmed. In the crystals, both subunits lie close to the membrane surface, attached to it by a part protruding from the large subunit.

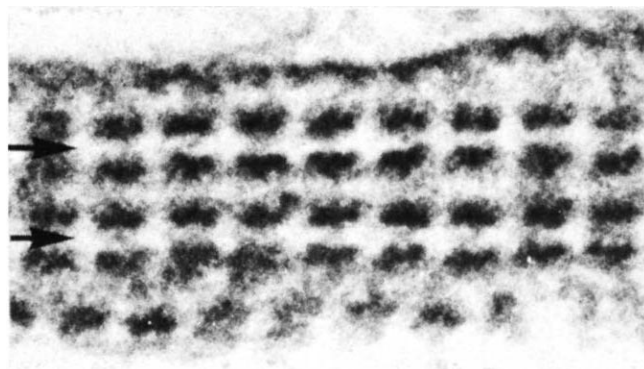
### Lizard ribosome crystals

The crystalline sheets of ribosomes which develop in the oocytes of the lizard *Lacerta sicula* during its winter hibernation period<sup>12</sup>, were used for this study. Each sheet is composed of two layers of ribosomes which are continuous with the cytoplasm and are bordered on either side by extended, flattened, vesicular membranes similar in appearance to the cisternae of the endoplasmic reticulum. In each layer of a sheet the ribosomes present the same surface to the membrane against which they are juxtaposed, and are arranged as tetramers in the space group P4 ( $a=595 \text{ \AA}$ ) (ref. 13). The crystalline material is inactive *in vivo*, but seems to be competent in protein synthesis when isolated and tested in a cell-free system<sup>14</sup>.

Face-on and edge-on views of the sheets are shown in Fig. 1. A detailed description of the packing of the ribosomes seen there and of the crystallographic relations between the layers of a sheet has been given elsewhere<sup>13</sup>. Face-on views (Fig. 1*a*) looked at from an appropriate glancing angle, show either tetramers or single ribosomes to line up in rows. When, in the edge-on views (Fig. 1*b*), the tetramers or the single ribosomes superimpose, they give rise to characteristic patterns of dashed (tetramer) or dotted (single ribosome) lines.

The membranes are most obvious in the edge-on views. They are separated from the densely staining parts of

**Fig. 2** Edge-on view of a six-layer stack of sheets formed by aggregation of three single sheets (each of two layers of ribosomes) in a medium of low ionic strength (50 mM KCl, 5 mM  $MgCl_2$ , 0.25 M sucrose, 50 mM triethanolamine-HCl, pH 7.6) containing 0.25% Triton. The zones from which the membranes have been extracted are indicated by the arrows. The other, darker, zones correspond to the region between the two layers of a sheet. Section  $\sim 2000 \text{ \AA}$  thick ( $\times 150,000$ ). Stacks of sheets formed artificially in this way have the same appearance as the 'three-dimensional crystals' of ribosomes which develop, in the absence of membranes, in live chick embryos when they are cooled<sup>15</sup>.



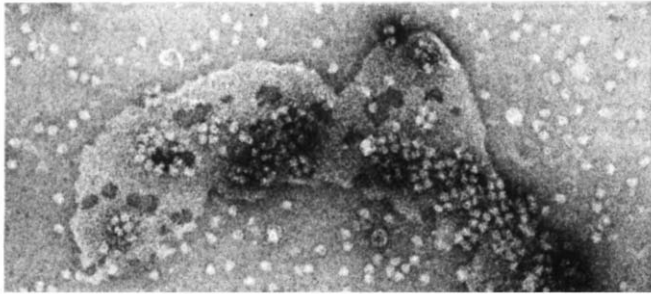


**Fig. 3** Single ribosomes and tetramers attached to membrane fragments after high salt treatment; negatively stained in uranyl acetate ( $\times 55,000$ ). The following steps were carried out at  $4^\circ\text{C}$ . The cytoplasm from about 50 selected previtellogenic oocytes were carefully opened out under a dissecting microscope into about  $50\ \mu\text{l}$  of low salt medium (50 mM KCl, 5 mM  $\text{MgCl}_2$ , 0.25 M sucrose, 50 mM triethanolamine-HCl, pH 7.6), stirred vigorously, then centrifuged at  $\sim 300g$  for 10 min to produce a pellet consisting almost entirely of large aggregates of ribosome sheets and membranes. This pellet was resuspended in  $50\ \mu\text{l}$  of high salt medium (500 mM KCl, 5 mM  $\text{MgCl}_2$ , 0.25 M sucrose, 50 mM triethanolamine-HCl, pH 7.6), held for 15 min, and then centrifuged at higher speed to remove any large contaminating material. The supernatant, containing the freed ribosomes and membranes was divided into two equal portions, one of which was dialysed against the low salt medium for several hours. Both portions were subsequently examined together in the microscope. Only the dialysed portion contained membrane-bound ribosomes. The few mitochondrial membranes present in these solutions, and erythrocyte ghosts which had been added to them before dialysis, showed no signs of attachment.

the crystalline ribosomes by a narrow, but distinct, zone relatively free of stained material. A zone of the same width is also observed when the membranes have been partially dissolved, indicating that osmotic effects are not responsible for its appearance or its width. No gap corresponding to this zone is found, however, between ribosomes and membranes in the non-crystalline regions. These ribosomes always seem to be more closely attached, as do those on the endoplasmic reticulum.

### Biochemical findings

The stain-depleted zone could be taken to indicate that the ribosome crystals are not attached to the membranes but are held apart, for example, by electrostatic forces. Other evidence favoured direct attachment, however: it was not possible to separate the components in detergent-free media of near physiological composition by normal mechanical means. In addition, the appearance of membrane-extracted stacks of sheets, which sometimes form in the presence of the detergent, Triton X-100 (see Fig. 2), seemed to imply that this zone contained some matter.

Two types of experiment gave more compelling evidence. In the first (Fig. 3) the KCl concentration was varied. It was found that the ribosome sheets, which seemed to be strongly attached to the membranes in solutions containing 5 mM  $\text{MgCl}_2$  at KCl concentrations of about 100 mM or less, were all released without difficulty, and dissociated into single ribosomes and subunits, when it was raised to 500 mM. Furthermore, the released ribosomes were competent in attaching specifically to fragments of the same membrane when the KCl concentration was brought down again. As Fig. 3 shows, many, but not all, of the ribosomes which attached on lowering the KCl concentration tended to associate to form tetramers; the crystal bonding between tetramers was not re-established. In the second experiment (Fig. 4), ribosome sheets which had been isolated from the membranes by detergent treatment<sup>13</sup>, were incubated with vesicles of lizard liver endoplasmic reticulum from which

the bound ribosomes had been removed. A large proportion of the surfaces of all sheets then became covered by membranes, as would be expected if the ribosomes composing them were orientated so that their salt-sensitive attachment sites were exposed and available for interaction. A strong association is suggested by the observations that most of the vesicles are drawn out in single membrane layers and that in places where they are only on one side they cause the crystal to bend.

I conclude that the ribosomes are directly attached to the membranes through a salt-sensitive linkage which may well be the same linkage that binds them to the endoplasmic reticulum.

### Analysis of isolated sheets

To investigate the three-dimensional structure of the ribosomes in the sheets they were isolated from the membranes as in ref. 13, placed on electron microscope grids and negatively stained with uranyl acetate. Micrographs were then taken of them tilted at angles between  $0^\circ$  and  $76^\circ$  to the incident 100-kV electron beam.

Fourier methods<sup>17,18</sup> were used to analyse and combine the data from the micrographs. The Fourier transform of one layer of ribosomes is a two-dimensional lattice of lines along which the phases and amplitudes vary continuously. The Fourier transform of an isolated sheet therefore consists of two such lattices, one of which is



**Fig. 4** Isolated crystalline sheets of ribosomes, (a), were incubated with vesicles of endoplasmic reticulum (b), giving the result, (c) ( $\times 40,000$ ). Vesicles of endoplasmic reticulum were prepared at  $4^\circ\text{C}$  by a procedure similar to that given in ref. 16. Two lizard livers were homogenised in about twice the volume of a medium containing 0.25 M sucrose, 50 mM triethanolamine-HCl, pH 7.6, and centrifuged twice at 15,000 r.p.m. ( $\sim 20,000g$ ) in a M.S.E. 3X6.5 titanium swing-out rotor, discarding the pellet and scum at the top on each occasion. The supernatant was then layered on to a discontinuous gradient of 1.5 M and 2.0 M sucrose in 50 mM KCl, 5 mM  $\text{MgCl}_2$ , 50 mM triethanolamine-HCl, pH 7.6, and spun at 42,000 r.p.m. ( $\sim 150,000g$ ) for 20 h, using the same rotor. The slightly opalescent 'rough microsome fraction' was withdrawn from the region near the 1.5 M/2 M sucrose interface and mixed with an equal volume of a high salt medium containing puromycin so that the final concentration was 500 mM KCl, 5 mM  $\text{MgCl}_2$ , 0.75 M sucrose, 50 mM triethanolamine-HCl, 1 mM puromycin, pH 7.6. This mixture was incubated at  $22^\circ\text{C}$  for 30 min to release the ribosomes and then passed through the same sucrose gradient as previously. The ribosome-stripped vesicle fraction was removed from the second centrifugation at a concentration of  $\sim 4\ \text{mg}$  of membrane protein per ml. The vesicle preparation was mixed with an equal volume of isolated ribosome sheets in 50 mM KCl, 5 mM  $\text{MgCl}_2$ , 0.25 M sucrose, 50 mM triethanolamine-HCl, pH 7.6, prepared as before<sup>13</sup>, and incubated for 6 h at  $0^\circ\text{C}$  before fixation, embedding and sectioning.

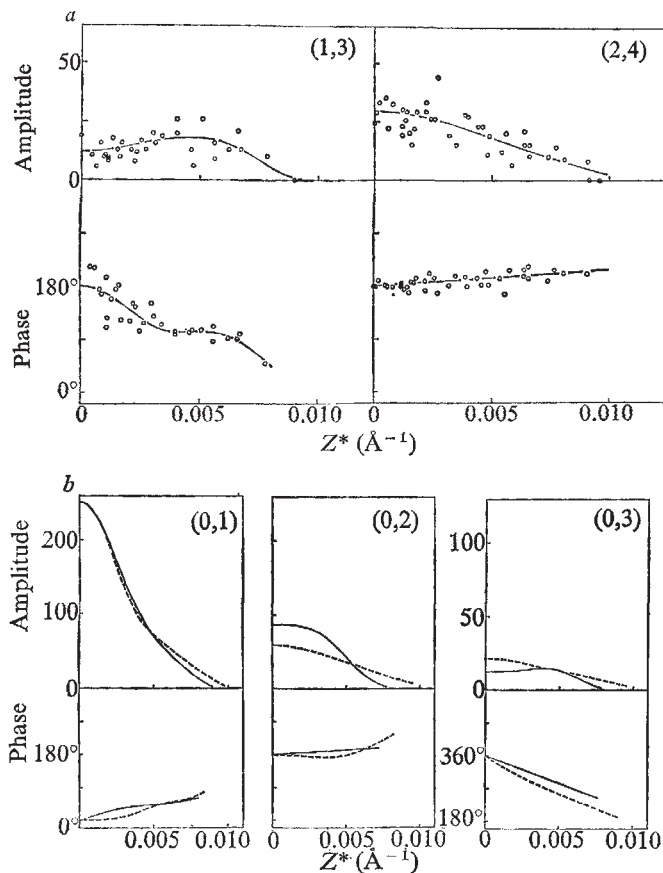


**Fig. 5** *a*, Values of calculated amplitudes and phases along two typical lattice lines, plotted as a function of distance ( $Z^*$ ) from their centres. In this space group the Friedel relationship gives the corresponding values for negative  $Z^*$ . Continuous curves drawn through the points and sampled every  $0.002 \text{ \AA}^{-1}$  give the data on which the three-dimensional map is based. The average phase error, based on comparison of single phase measurements against all others within a small range of  $Z^*$ , is less than  $20^\circ$ . Micrographs were taken with a goniometer stage, using bent support grids to achieve the highest tilt angles. They were densitometered and analysed as in ref. 13. The information was combined as in ref. 18. No corrections for effects of defocus were needed at this resolution. *b*, Amplitudes and phases calculated for the  $(0,k)$  lattice lines from the tilting experiments (full line) and from edge-on views of superimposed tetramers in  $\sim 2,000\text{-\AA}$  thick sections (broken line). The data obtained from the edge-on views have been adjusted to give the best fit with the data from the tilting experiments, the difference between positive and negative staining being accounted for by a  $180^\circ$  phase change. The amplitude scale factor and phase origin adjustment needed to fit the two sets of data were used to correct the variation along the  $(0,0)$  lattice line, which the edge-on view gives directly.

upside-down and rotated by a specific amount with respect to the other, depending on the crystallographic relationship between the two layers. Hence, each micrograph gives two sections through the three-dimensional Fourier transform of one layer.

Sixteen micrographs (32 different views of one layer) were needed to give continuous curves of phase and amplitude along all of the 25 crystallographically independent lattice lines, except for the line through the origin, out to a resolution of  $90 \text{ \AA}$ . Two such curves are shown in Fig. 5*a*. Several micrographs from a given tilt series were suitable for data collection since radiation damage was not a limiting factor.

Optical diffraction patterns from micrographs of negatively stained and (sectioned) positively stained isolated sheets were similar, indicating that at this low resolution, except for the reversal in contrast, positively stained and negatively stained sheets would provide roughly

equivalent maps of the structure. The approximate form of the lattice line through the origin could therefore be determined from sectioned material by calculating the Fourier transform of an edge-on view of one layer. The correct scale of the amplitudes and the origin adjustment for the phases along this lattice line were then found by comparing data, as in Fig. 5*b*.

By sampling the continuous variation of the complete transform at suitably fine intervals ( $0.002 \text{ \AA}^{-1}$ ) along the lattice lines, a three-dimensional map of the ribosomes in one layer was calculated.

### Three-dimensional map

Figure 6 shows a tetrameric unit from the three-dimensional map, viewed so that the juxtaposed membrane, if it were present, would lie underneath, and also a single ribosome from this unit, viewed parallel to the plane of the array. The contours map out the negative stain-excluding regions only. Therefore they are insensitive to differences of composition within the ribosome and do not show up areas of RNA or protein into which the negative stain may have penetrated.

Particularly noticeable in Fig. 6*a* is a region within the ribosomes which looks like a hole, and so probably represents that part where the large and small ribosomal subunits are most widely separated. The shape and dimensions of the matter surrounding this region resemble features observed in micrographs of isolated eukaryotic ribosomes and of their isolated subunits<sup>19,20</sup>. A detailed comparison, and arguments based on molecular weight estimates<sup>21</sup>, indicate that the two subunits lie side by side, and suggest that the ribosome can be partitioned as shown, with the large subunit closest to the centre of the tetramer. The line dividing the subunits seems to follow the path in which the inner contours come closest together and connect the 'hole' to the outside, but its exact position cannot be determined from this low resolution map.

Figure 6*b*, the view of a single ribosome along the direction of this path, emphasises another feature of the other map—a narrow protrusion on the large subunit

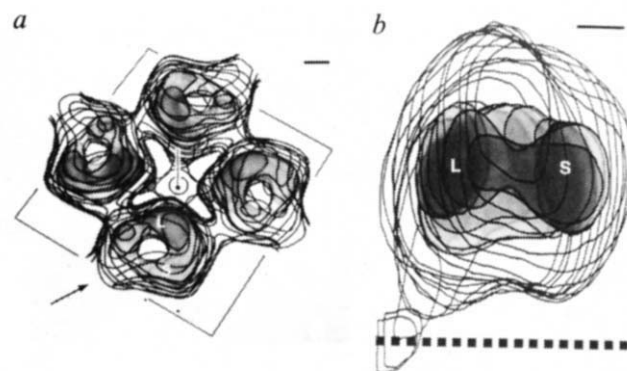


**Fig. 6** Views of *a*, a tetramer and *b*, a single ribosome emphasising the dominant features of the three-dimensional map. The negative contours, representing the stain excluding parts, have been drawn at two levels ( $-2$  and  $-6$  in a scale  $0$  to  $-10$ ) and the region within the inner contours has been shaded. The tetramer is orientated so that the juxtaposed membrane would lie underneath (right-handed configuration<sup>13</sup>); it is upside-down in comparison with the usual orientation on microscope grids of isolated tetramers and tetramers in p4 arrays<sup>22</sup>, where the ribosomes present 'left featured frontal' views<sup>19,20</sup>; thus the small subunit (S) is on the anticlockwise side, and the large subunit (L) on the clockwise side, of the path (arrowed) connecting the 'hole' to the outside. The single ribosome is viewed from the direction indicated by the arrow; the feature protruding from it was estimated, independently of the map, to extend as far ( $\pm 15 \text{ \AA}$ ) as the dotted line. Scale bars represent  $50 \text{ \AA}$ .

extending towards the central fourfold axis. From the configuration of the group of four of them, it seems that the ribosomes of a tetramer touch in the region close to the central fourfold axis, as well as at a higher radius. These protrusions are unlikely to be something peculiar to ribosomes which crystallise, since the tetramers can be formed *in vitro* from ribosomal subunits released from polysomes<sup>22</sup>. Nor are they likely to be membrane proteins, since another explanation would then be required for the identical packing of ribosome tetramers in the non-membrane associated stacks of sheets found in chick embryos when they are cooled<sup>15</sup>. They are therefore most probably normal components of the large subunits.

### Membrane attachment

Edge-on views of stacks of sheets (Fig. 2) were used to derive, independently of the three-dimensional map, the distance reached by the protrusions in the direction of the membrane. In the membrane-extracted zones of these stacks the protrusions show up as slightly denser areas between the dashed lines formed by the tetramers, and presumably extend halfway into the zones. The half-way distance was estimated from projection maps calculated from Fourier transforms of these views, using the data on which the three-dimensional map is based to obtain the correct scale and to define the centre of a layer. The result of the estimate, the furthest distance reached by the protrusions in the direction of the membrane, is indicated by the dotted line drawn in Fig. 6b. The position of this line is consistent with the details in the map.

The line in Fig. 6b could also represent the surface of the membrane with which the crystalline ribosomes are associated *in vivo*, since the open space between the protrusions would then give a zone of the same width as seen in Fig. 1b. No additional material is required to span the space. Therefore the protrusions must be the links by which the crystalline ribosomes establish contact with sites on the membrane surface.

It seems unnecessary to draw a distinction in mode of attachment between the crystalline and non-crystalline membrane-bound ribosomes. The closer association with

the membrane of the latter could be due to some freedom of movement of the ribosomes about their attachment site when they are no longer constrained by the crystal bonding.

It is possible that membrane-bound ribosomes are attached by the same mode—some distance from the body of the ribosome—during the initial stages of protein synthesis. A wide separation between the site where the large subunit binds and the emerging polypeptide should allow the polypeptide freedom of motion relative to the highly fluid<sup>23,24</sup> endoplasmic reticulum, without greatly disturbing its proximity or orientational disposition. Thus, the main function of this type of attachment could be to give the molecules in the membrane and the protein being synthesised a good chance to interact.

I thank Nichol Thompson for cutting the sections, Dr L. Amos for some computer programs and Drs C. Taddei, R. Henderson and M. Bretscher for helpful discussions. The Philips Application Laboratory Cambridge, kindly made available the goniometer version of their EM400 electron microscope for the tilting experiments.

Received 13 May; accepted 8 July 1977.

- 1 Sjekevitz, P. & Palade, G. E. *J. biophys. biochem. Cytol.* **7**, 619–644 (1960).
- 2 Redman, C. M., Sjekevitz, P. & Palade, G. E. *J. biol. Chem.* **241**, 1150–1158 (1966).
- 3 Adelman, M. R., Sabatini, D. D. & Blobel, G. *J. Cell Biol.* **56**, 206–229 (1973).
- 4 Milstein, C., Brownlee, G. G., Harrison, T. M. & Mathews, M. B. *Nature new Biol.* **239**, 117–120 (1972).
- 5 Blobel, G. & Dobberstein, B. *J. Cell Biol.* **67**, 835–851 (1975).
- 6 De Villiers-Thierry, A., Kindt, T., Scheele, G. & Blobel, G. *Proc. natn. Acad. Sci. U.S.A.* **72**, 5016–5020 (1975).
- 7 Wirth, D. F., Katz, F., Small, B. & Lodish, H. F. *Cell* **10**, 253–263 (1977).
- 8 Sabatini, D. D., Tashiro, Y. & Palade, G. E. *J. molec. Biol.* **19**, 503–524 (1966).
- 9 Redman, C. M. & Sabatini, D. D. *Proc. natn. Acad. Sci. U.S.A.* **56**, 608–615 (1966).
- 10 Malkin, L. I. & Rich, A. *J. molec. Biol.* **26**, 329–346 (1967).
- 11 Blobel, G. & Sabatini, D. D. *J. Cell Biol.* **45**, 130–145 (1970).
- 12 Taddei, C. *Expl Cell Res.* **70**, 285–292 (1972).
- 13 Unwin, P. N. T. & Taddei, C. *J. molec. Biol.* **114**, 491–506 (1977).
- 14 Taddei, C., Gambino, R., Metafora, S. & Monroy, A. *Expl Cell Res.* **78**, 159–169 (1973).
- 15 Byers, B. *J. molec. Biol.* **26**, 155–167 (1967).
- 16 Adelman, M. R., Blobel, G. & Sabatini, D. D. *J. Cell Biol.* **56**, 191–205 (1973).
- 17 DeRosier, D. J. & Klug, A. *Nature* **217**, 130–134 (1968).
- 18 Henderson, R. & Unwin, P. N. T. *Nature* **257**, 28–32 (1975).
- 19 Nonomura, Y., Blobel, G. & Sabatini, D. D. *J. molec. Biol.* **60**, 303–323 (1971).
- 20 Lake, J. A., Sabatini, D. D. & Nonomura, Y. in *Ribosomes* (eds Nomura, M., Tissières, A. & Lengyel, P.) 543–557 (Cold Spring Harbor Laboratory Press, New York, 1974).
- 21 Wool, I. G. & Stöffler, G. in *Ribosomes* (eds Nomura, M., Tissières, A. & Lengyel, P.) 417–460 (Cold Spring Harbor Laboratory Press, New York, 1974).
- 22 Byers, B. *Proc. natn. Acad. Sci. U.S.A.* **68**, 440–444 (1971).
- 23 Rogers, M. J. & Strittmatter, P. *J. biol. Chem.* **249**, 895–900 (1974).
- 24 Ojakian, G. K., Kreibich, G. & Sabatini, D. D. *J. Cell Biol.* **72**, 530–551 (1977).

## *In vitro* synthesis of infectious DNA of murine leukaemia virus

Ellen Rothenberg, David Smotkin,  
David Baltimore & Robert A. Weinberg

Department of Biology and Center for Cancer Research, Massachusetts Institute of Technology, Cambridge, Massachusetts 02139

*DNA synthesised in vitro by purified virions of murine leukaemia virus is infectious. Neither RNA nor protein is required for infectivity. Transfection with reverse transcriptase product shows a single-hit dose response and results in the production of complete, infectious virus.*

THE discovery of reverse transcriptase in virions of retroviruses<sup>1,2</sup> provided a system for studying the viral DNA synthesis which was known to be essential early in infection<sup>3,4</sup>. Until recently, however, most groups studying reverse transcription *in vitro* found the DNA products to be small relative to the size of the RNA templates. Thus it was not known whether virions could make a complete copy of the

viral genome without the intervention of cellular factors.

Recent studies have improved reaction conditions so as to allow detergent-disrupted virions to synthesise DNA molecules up to 8,000–9,000 nucleotides long, the length of the viral genome RNA which serves as template<sup>5–7</sup>. It has been possible to synthesise very long DNA transcripts in the 'endogenous reaction' without sacrificing the specificity of initiation: the longest products made by virions of Moloney murine leukaemia virus (M-MuLV) apparently share the unique initiation site and tRNA<sup>Pro</sup> priming mechanism used by the shorter transcripts<sup>8,9</sup>. Since the longest transcripts also migrate as a discrete species close to genome length in Agarose gel electrophoresis, it seemed possible that they could be biologically active. We report here that infectious DNA can be synthesised *in vitro* by purified virions of M-MuLV.